

# Successive Computations of an ODF While Measuring its Corresponding PDFs with Respect to Progressively Locally Refined Spherical Grids

H. Schaeben<sup>1</sup>, R. Hielscher<sup>1</sup>, J. J. Funderberger<sup>2</sup>, D. Potts<sup>3</sup>, J. Prestin<sup>4</sup>

<sup>1</sup>*Geoscience Mathematics and Informatics, Freiberg University of Mining and Technology, BvCotta Str. 2, D-09596 Freiberg, Germany*

*E-mail: schauben@geo.tu-freiberg.de*

<sup>2</sup>*Laboratoire d'Etude des Textures at Application aux Matériaux, UMR CNRS 7078, Université de Metz, France*

<sup>3</sup>*Mathematics, Chemnitz University of Technology, Germany*

<sup>4</sup>*Mathematics, Lübeck University, Germany*

## 1. Abstract

Due to a novel method of pole intensity to orientation density inversion applying radial basis functions and an implementation employing fast Fourier transform algorithms for  $\mathbb{S}^2$ ,  $\mathbb{S}^2 \times \mathbb{S}^2$ , and  $\text{SO}(3)$  it is now possible to process intensity data arbitrarily scattered on the pole sphere and successively compute numerical approximations of an ODF explaining the data while they are being measured. Therefore we suggest an adaptive successive refinement of an initial coarse uniform grid to a locally refined grid where the progressive refinement corresponds to the pattern of preferred crystallographic orientation. At each level of refinement an ODF is computed, and the refinement is terminated if some stopping rule is accomplished.

## 2. Mathematics of Texture Analysis

The major mathematical problem of the analysis of crystallographic preferred orientation (“texture analysis”) is the inversion of experimental “pole figures”, i.e. sampled spherical distributions (PDFs) of crystallographic axes  $h \in \mathbb{S}^2$ , into an orientation density function (ODF)  $f$  defined on  $\text{SO}(3)$ . The relationship of an ODF  $f$  and its corresponding PDFs  $P(h,r)$  is basically modelled by the one-dimensional totally geodesic Radon transform

$$Rf(h, r) = \frac{1}{2\pi} \int_{G(h,r)} f(g) dg, \quad (h, r) \in \mathbb{S}^2 \times \mathbb{S}^2, \quad (1)$$

which associates to an orientation probability density function  $f$  on  $\text{SO}(3)$  its mean values along the one-dimensional geodesics (Hopf “fibres”)

$$G(h, r) = \{g \in \text{SO}(3) \mid gh = r, (h, r) \in \mathbb{S}^2 \times \mathbb{S}^2\}.$$

Then the  $h$ -pole density function is defined as

$$P(h, r) = \frac{1}{2} (Rf(h, r) + Rf(h, -r)) = \chi f(h, r), \quad (2)$$

which we also call basic crystallographic X-ray transform even though it does not depend on the radiation used for diffraction. Notationally we do not distinguish between experimentally accessible pole figures and the basic crystallographic X-ray transform, which differ just by a summation over crystallographically symmetrically equivalent directions.

In practice, the problem is to recover a reasonable approximation of the orientation probability density function  $f$  from experimental intensities

$$l_{ij} = l(h_i, r_{ji}) = a(h_i)P(h_i, r_{ji}) + b(h_i), \quad j_i = 1, \dots, J_i, \quad i = 1, \dots, I \quad (3)$$

modelled by pole probability density functions  $P$  with constants  $a(h_i), b(h_i) \in \mathbb{R}$  depending on the crystal form. The indices indicate that there is no regular grid of positions  $(h_i, r_{ji})$  imposed but that the specimen positions  $r_{ji}$  may depend on the crystal form  $h_i$  and may be different for each crystal form.

However, in contrast to the inverse Radon problem the PDF-to-ODF inversion problem does not possess a unique solution, but additional modelling assumptions are required. Canonical modelling assumptions seem to include the non-negativity of both orientation and pole density functions as well as their smoothness implied by the characterization of the range of the Radon transform.

### 3. Numerics of Texture Analysis

Our novel method to resolve the PDF-to-ODF inversion problem (Hielscher, 2007, Hielscher and Schaeben, 2006) is to solve the non-linear regularization problem

$$\tilde{c} = \arg \min \sum_{i=1}^I \sum_{j=1}^{J_i} \left\| \sum_{m=1}^M a(h_i) C_m R \psi_k(g_m h_i, r_{ij}) + b(h_i) - l_{ij} \right\|^2 + \lambda \left\| \sum_{m=1}^M C_m \psi_k(\circ g_m^{-1}) \right\|_{H(SO(3))}^2, \quad (4)$$

where  $\lambda$  is the parameter of regularization weighting the penalty term, applying radial basis functions  $\psi_k(\circ g_m^{-1})$  defined on  $SO(3)$  and an implementation employing fast Fourier transform algorithms. Due this method we get rid of obsolete restrictions such as seriously bounded series expansion degree, seriously bounded total number of components, regular spherical grid of measurements on the pole sphere, weak to moderate textures, large cpu times etc.

To solve the problem Eq. (4) numerically methods of fast matrix-vector multiplication are combined with iterative methods. Fast Fourier transforms are an option for the fast matrix-vector multiplication, alternatively multipole or multigrid methods may be used. The modified steepest descent algorithm provides an iterative solution for the non-negative constrained optimization problem, and so do Richardson-Luci, gradient projection residual norm (GPRN) and gradient projection residual norm conjugated gradients (GPRNCG) method (cf. Bardsley and Vogel, 2003).

Since it is now possible to process intensity data arbitrarily scattered on the pole sphere and successively compute numerical approximations of an ODF explaining the data while they are being measured, we suggest a new experimental strategy, which depends on the texture being measured itself. In particular we suggest an adaptive successive refinement of an initial coarse uniform grid to a locally refined grid where the progressive refinement corresponds to the pattern of preferred crystallographic orientation. At each level of refinement an ODF is computed, and the refinement is terminated if some stopping rule is accomplished.

### 4. Practical Example

Figure 1 exemplifies the adaptive successive refinement of the experimental grid for the (001)-pole figure of a Molybdenum specimen with cubic crystal symmetry.

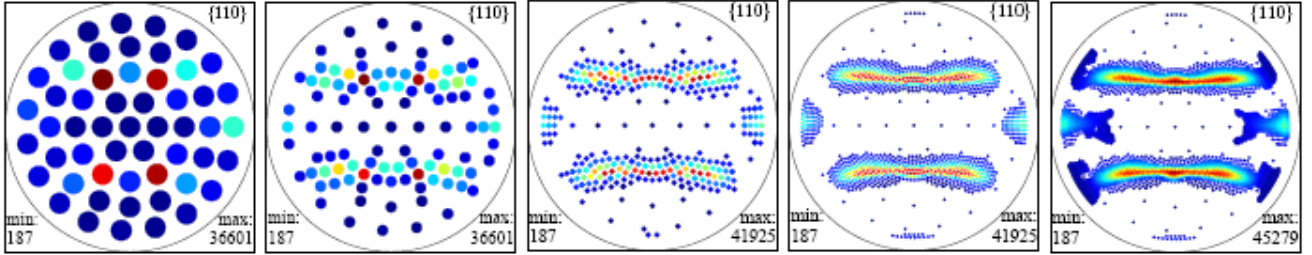


Fig. 1. Successive local refinement of an initially coarse grid

In Table 1 the parameters of the individual steps are summarized. Since the measurement time almost linearly increases with the number of measured diffraction intensities we conclude that we have time savings of about 40 percent in the third step of the successive refinement, and up to 75 percent or 150 hours (step five). The computational time for the PDF-to-ODF inversion was measured on a notebook with Intel Core 2 Duo processor with 1.86 GHz cpu frequency and 2 GB memory. Obviously, the computational time is negligible compared with the time savings during the measurement process. It should also be noted that the cpu time increases with a factor of  $2^3 = 8$  from one refinement to the next except for the last refinement as it depends only on the spatial resolution of the grid of  $SO(3)$  which is successively doubled, and not on the total number of measured intensities  $\bar{N}$ . In the last step a lack of memory caused additional computations and memory swapping. In case of sufficiently large memory the cpu time could be reduced from 31 hours to approximately 4 hours.

step	$\delta$	$\bar{N}$	$\bar{N}_{reg}$	mesns.time [h]	M	L	cpu time
1	$20^\circ$	216	288	0.60	21	23	3 sec
2	$10^\circ$	443	1,152	1.23	204	52	28 sec
3	$5^\circ$	1,621	4,608	4.50	1,493	108	209 sec
4	$2.5^\circ$	5,511	18,432	15.30	11,767	215	1600 sec
5	$1.25^\circ$	19,191	73,728	53.30	94,040	432	31 h

Table 1: Parameters for individual refinement and recalculation steps, including the resolution  $\delta$  of the grid of specimen directions of  $\mathbb{S}^2$ , the cumulative total number  $\overline{N}$  of measured diffraction intensities with respect to the locally refined grids, the total number  $\overline{N}_{\text{reg}}$  of diffraction intensities to be measured in a conventional experiment with a regular grid, the cumulative measurement time, the total number  $M$  of ansatz functions involved in the PDF-to-ODF inversion problem, the maximum order of harmonic series expansion (bandwidth)  $L$  of the ansatz functions, and the computational time to solve the PDF-to-ODF inversion problem with Core 2 Duo cpu with 1.86 GH cpu-frequency and 2 GB RAM.

## 5. Conclusions

The advantage of this experimental design is that it largely decreases the measuring time or makes best use of the available measuring time. It is especially well suited to capture, represent and analyse extremely sharp textures as in technical single crystals.

## 6. Acknowledgments

The authors, especially RH, gratefully acknowledge financial support by Deutsche Forschungsgemeinschaft, grant “high resolution texture analysis” (SCHA 465/15).

## 7. References

- Bardsley, J.M., Vogel, C.R., 2003. A nonnegatively constrained convex programming method for image reconstruction. *SIAM J. Sci. Comput* 25, 1326-1343.
- Hielscher, R., 2007. The Inversion of the Radon Transform on the Rotational Group and Its Application to Texture Analysis. Ph.D. Dissertation, Technische Universitaet Freiberg, Freiberg, Germany.
- Hielscher, R., Schaeben, H., 2006. A novel method to determine crystallographic preferred orientations from diffraction experiments. In: Proceedings of IAMG2006, Liège, Sep 3-8, 2006, CD S06-12, 1pp.